MAGNETIC AND MAGNETO-OPTICAL PROPERTIES OF Co-BASED MULTILAYERED FILMS PREPARED BY ELECTRON-BEAM EVAPORATION

Y. P. Lee,* B. J. Lee,** H. K. Park,*** S. K. Kim,** J. S. Kang,*** J. I. Jeong,*** and Y. M. Koo**
*Physics Department, Sunmoon University, Asan 336-840, Korea
**Pohang University of Science & Technology, Pohang 790-784, Korea
***Research Institute of Industrial Science & Technology, Pohang 790-330, Korea

ABSTRACT

The magnetic amd magneto-optical (MO) properties of Co-based multilayered (ML) films are known to vary sensitively according to the manufacturing methods and the film microstructures. Co/Pd and Co/Pt ML films with ultrathin layers of Co were prepared by alternating deposition in an ultrahigh-vacuum physical-vapor-deposition system. The individual layer thicknesses of the samples were estimated making use of the angular positions of x-ray diffraction peaks. The magnetic and MO properties were investigated, and correlated systematically to the structural parameters of the films. A Kerr spectrometer was self-manufactured to measure the MO properties such as Kerr rotation angle, ellipticity and reflectivity. The rms surface roughness was also measured using atomic force microscopy. Some of the samples showed good properties for MO medium, such as large perpendicular magnetic anisotropy and Kerr rotation, and perfect squareness of the magnetic hysteresis loop.

1. INTRODUCTION

Ferromagnetic/nonferromagnetic multilayered (ML) thin films have attracted wide attention as high-density magneto-optical (MO) media because of their large perpendicular magnetic anisotropy when the interfacial anisotropy exceeds the volume anisotropy. The vulnerability of rare-earth transition-metal amorphous alloys to oxidation and corrosion, and the needs for larger Kerr rotation angle at shorter wavelengths result in research on transition-metal/noble-metal ML thin films such as Co/Pd and Co/Pt[1-6].

Co/Pd and Co/Pt ML films were made with an ultrahigh-vacuum physical-vapor-deposition system at a deposition rate of < 0.1 - 0.4 Å/s. We observed the effects on the coercivity, magnetic anisotropy, Kerr rotation angle and Kerr ellipticity according to the Pd or Pt buffer layer and Pd or Pt sublayer thicknesses measured accurately by x-ray diffraction (XRD), and the microstructure of the ML film such as the texture, interfacial abruptness and surface roughness.

2. EXPERIMENT

Co/Pd MLs were deposited onto a Si substrate at 30 - 80°C under a pressure of 0.5 - 2.0 x 10^{-6} mbar (base pressure of 0.5 - 1.5 x 10^{-7} mbar) by alternating electron-beam and thermal evaporation of Co and Pd, respectively. Co/Pt MLs were deposited at 30 - 60°C under a pressure of 1 - 3 x 10^{-6} mbar (base pressure of 1 - 2 x 10^{-7} mbar) by alternating electron-beam evaporation. The deposition rates and sublayer thicknesses were monitored in-situ with single crystal quartz sensor (1% error) calibrated by XRD measurements. The structure of the ML films is $(t_{Pd\ or\ Pt} + t_{Co}) \times N / T_{Pd\ or\ Pt}$, where $t_{Pd\ or\ Pt}$ and t_{Co} are Pd- or Pt- and Co-sublayer

thickness, respectively, N is the number of the bilayers, and $T_{Pd\ or\ Pt}$ is the Pd or Pt buffer layer thickness. For Co/Pd MLs, t_{Co}, t_{Pd}, N and T_{Pd} were prepared to be in the ranges of 2 - 11 Å, 6 - 40 Å, 10 - 20 Å and 30 - 200 Å, respectively. Two series of the samples were prepared for Co/Pt MLs ; (Pt(10Å) / t_{Co}) x 15 / Pt(10Å) where t_{Co} is varied to be 2 - 12 Å, and (Pt(10Å) / Co(3Å)) x 15 / T_{Pt} where T_{Pt} is varied to be 10 - 500 Å.

The structural parameters and the compositions of the MLs were determined using an x-ray diffractometer (XRD)[7], transmission electron microscopy (TEM), atomic force microscopy (AFM) and Auger electron spectroscopy (AES). Magnetic properties were measured with a vibrating sample magnetometer and a torque magnetometer. MO Kerr effect of Co/Pd MLs was investigated with a Kerr loop tracer at the wavelength of 830 and 780 nm. For Co/Pt MLs, MO effect was measured with a self-manufactured Kerr spectrometer based on photoelastic modulation, whose wavelength range is 400 - 900 nm and whose maximum magnetic field is 15 kOe at a pole gap of 1", and a Kerr loop tracer at the wavelength of 780 nm.

3. RESULTS AND DISCUSSION

In the small-angle parts of XRD, the first, second and third satellite peaks were observed, as well as the existence of the first negative and positive peaks in the large-angle part, which indicates that the films have a compositionally modulated structure with sharp interfaces. The film texture turned out to be (111). This is also supported by cross-sectional TEM measurements. The rms surface roughness of Co/Pt MLs measured by AFM was increased with T_{Pt} from 5 Å at T_{Pt} = 10 Å to 11 Å at T_{Pt} = 500 Å as in Fig. 1. The grain size was also increased with T_{Pt}.

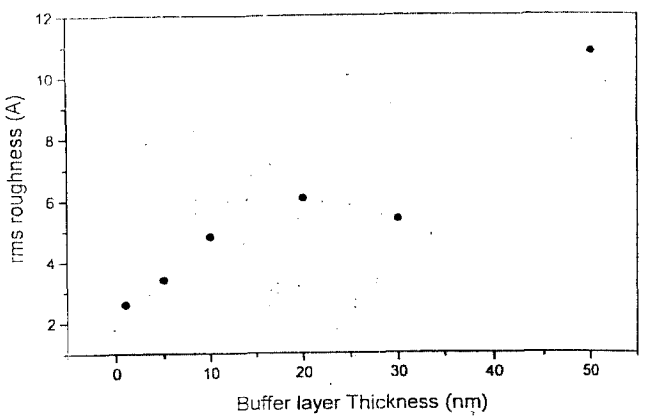

Fig. 1 rms roughness of Co/Pt MLs measured by AFM according to T_{Pt} (from 10 to 500 Å)

The change in coercivity (H_c) according to the structural parameters of Co/Pd MLs is described in Fig. 2. The coercivity is decreased as t_{Pd}/t_{Co} is increased. Figure 2(b) shows that a remarkable increase in coercivity from 1901 to 4723 Oe occurs when T_{Pd} is changed from 62.5 to 136 Å on which a ML of 6.2 Å Pd / 1.9 Å Co was deposited. A further increase in T_{Pd} decreases the coercivity to 3150 Oe. This high coercivity of 4723 Oe suggests that we consider the effects of the atomic distributions of Co and Pd at interfaces on the magnetic properties. The final decrease in coercivity might be due to an excessive amount of the nonferromagnetic element, Pd, in the film at a large T_{Pd}. The change in H_c of Co/Pt MLs according to T_{Pt} is described in Fig. 3 which shows that a remarkable increase to 4000 Oe when T_{Pt} is changed to 300 Å. The saturation magnetization (M_s) of Co/Pt MLs is decreased with T_{Pt}.

In order to estimate the interfacial and volume anisotropies of Co/Pd MLs, we plot $k_{eff} \cdot t_{Co}$ as a function of t_{Co}, where k_{eff} is effective magnetic anisotropy, in Fig. 4. For the samples

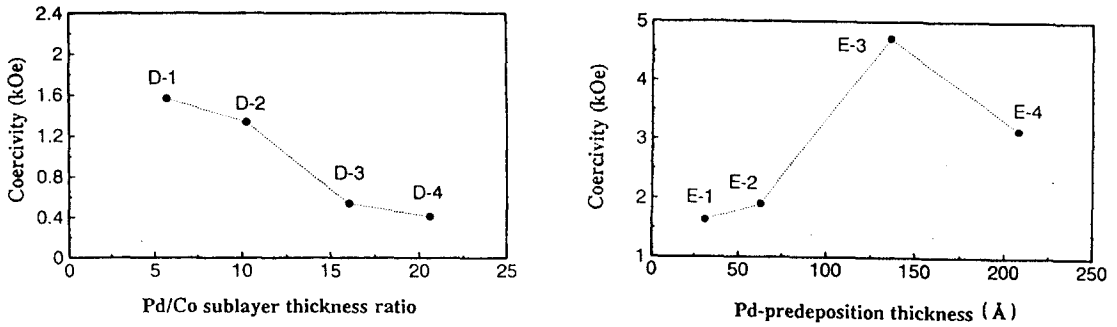

Fig. 2 Coercivity of Co/Pd MLs according to sublayer and Pd buffer layer thicknesses. Coercivity vs (a) t_{Pd}/t_{Co} , and (b) T_{Pd}.

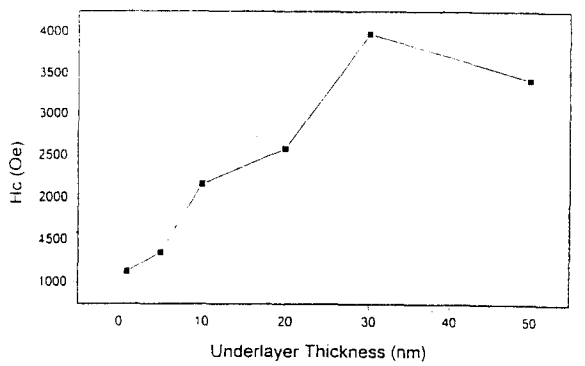

Fig. 3 Coercivity of Co/Pt MLs according to T_{Pt}

which had a Pd buffer layer (the data around t_{Co}^{tr} at which $k_{eff} = 0$) , $k_s = 0.72 \pm 0.12$ mJ/m^2 and $k_v = -1.76 \pm 0.21$ MJ/m^3 using a linear least-square fit. The deviated data of very small t_{Co} is excluded in the fit because these samples were not prepared with abrupt interfaces owing to the nonuniform growth of very thin sublayers. It should be noticed that our values for k_s and $-k_v$ are large. Bennet *et al.*[8] predicted a maximum k_s of 0.79 mJ/m^2 at room temperature

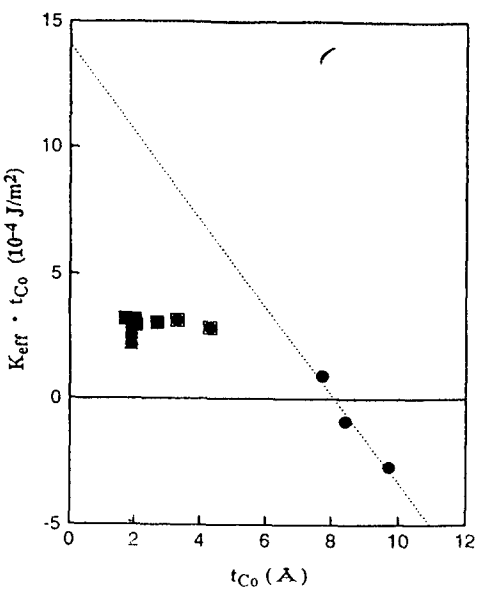

Fig. 4 k_{eff} times t_{Co} of Co/Pd MLs as a function of t_{Co}. The different symbols denote the different groups of samples. The dashed line is the least-square fit for the samples of larger t_{Co}.

using a pair model. Our k_s of 0.72 mJ/m^2 is a little smaller than this value probably because the prepared ML's have slight deviations from perfect abruptness at the interfaces. Our value of - k_v is larger than that for pure Co ($2\pi M_s^2$ = 1.29 MJ/m^3), which is interpreted as the increase in demagnetization contribution due to induced polarization of Pd by Co. The torque curves for all the samples of (Pt(10Å) / Co(3Å)) x 15 / T_{Pt} show positive effective anisotropy, and the perpendicular magnetic anisotropy is enhanced with $T_{Pt} \leq 200$ Å. On the other hand, the samples of (Pt(10Å) / t_{Co}) x 15 / Pt(10Å) show negative one when $t_{Co} > 4$ Å.

Figure 5 shows Kerr rotation angle (θ_k) vs t_{Pd}/t_{Co} of Co/Pd MLs without Pd buffer layer, which have 100% remanent magnetization, at 780 and 830 nm. The angles at shorter wavelength are larger than those at longer wavelength. Figure 6 (a) is the θ_k spectra from 450 to 850 nm of (Pt(10Å) / t_{Co}) x 15 / Pt(10Å) samples according to t_{Co}, showing larger θ_k

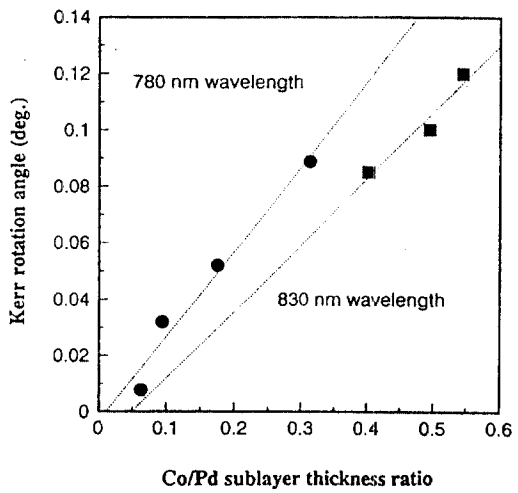

Fig. 5 θ_k's at 780 and 830 nm vs t_{Co}/t_{Pd} for Co/Pd MLs with 100% remanent magnetization and without Pd buffer layer

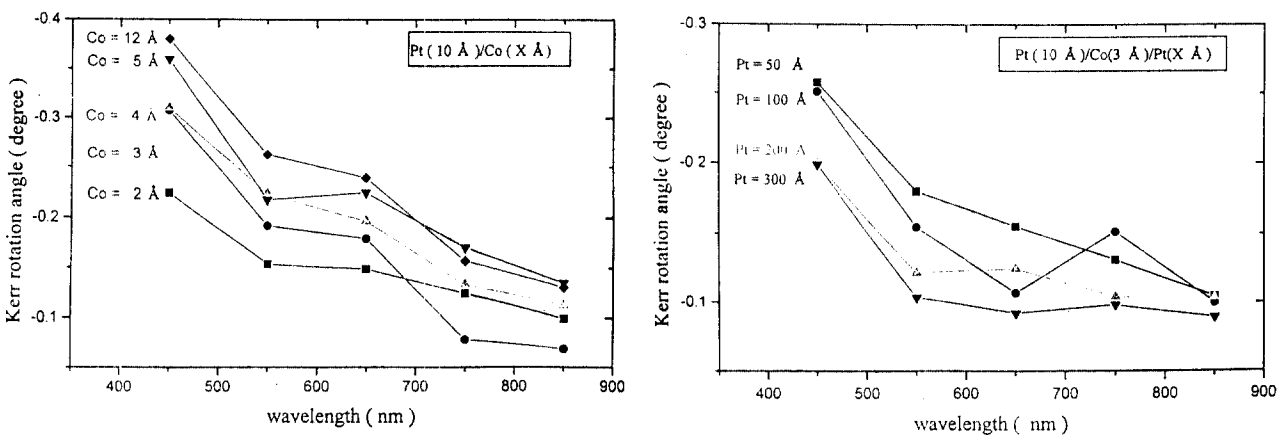

Fig. 6 θ_k spectra of Co/Pt MLs. (a) (Pt(10Å) / t_{Co}) x 15 / Pt(10Å), and (b) (Pt(10Å) / Co(3Å)) x 15 / T_{Pt}.

at larger t_{Co} and shorter wavelength, and Fig. 6 (b) is those of (Pt(10Å) / Co(3Å)) x 15 / T_{Pt} samples according to T_{Pt}, showing larger θ_k at smaller T_{Pt} and shorter wavelength. The variation of t_{Co} turns out to be more effective for the enhancement of θ_k than that of T_{Pt}. (Pt(10Å) / t_{Co}) x 15 / Pt(10Å) MLs also revealed worse squareness of the polar Kerr hysteresis loop and small remanent θ_k with increasing t_{Co}. The reflectivity (R) spectra of (Pt(10Å) / Co(3Å)) x 15 / T_{Pt} samples are also measured according to T_{Pt} (Fig. 7). The highest reflectivity is observed at T_{Pt} = 200 Å, with a maximum of 78% at 650 nm. Figure of merit (R θ_k) which indicates the signal-to-noise ratio of MO medium is also evaluated at various T_{Pt}'s and wavelengths for (Pt(10Å) / Co(3Å)) x 15 / T_{Pt} samples as in Fig. 8, showing the best figure of merit at 450 nm and a maximum of 0.19° at T_{Pt} = 50 Å.

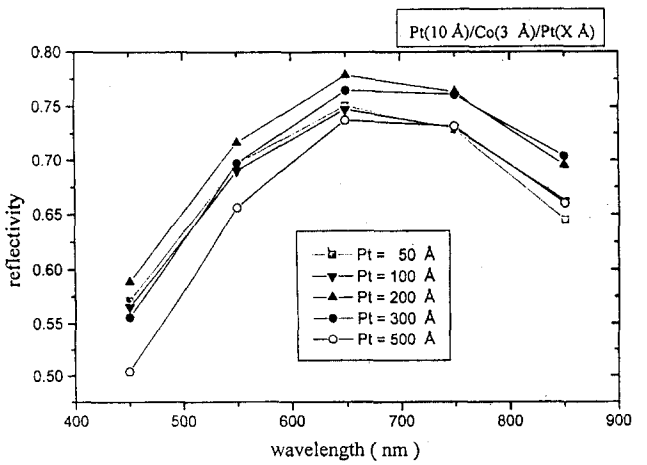

Fig. 7 R spectra of (Pt(10Å) / Co(3Å)) x 15 / T_{Pt} samples according to T_{Pt}

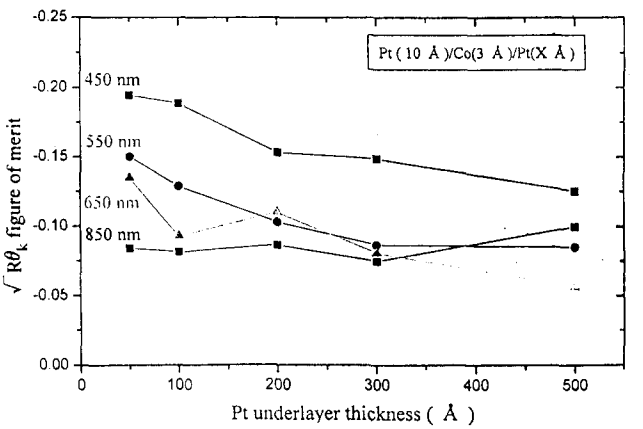

Fig. 8 Figure-of-merit data of (Pt(10Å) / Co(3Å)) x 15 / T_{Pt} samples according to T_{Pt} and wavelength

4. CONCLUSIONS

ML films with ultrathin sublayer thicknesses and sharp interfaces were prepared using an ultrahigh-vacuum physical-vapor-deposition system. Sublayer thicknesses and surface roughness were measured accurately by XRD and AFM, respectively. For Co/Pd MLs, a remarkable increase in coercivity from 1901 to 4723 Oe occurred when T_{Pd} was shifted from 62.5 to 136 Å. Samples with Pd buffer layer showed $k_s = 0.72$ mJ/m^2, which is very close to the maximum k_s of 0.79 mJ/m^2 predicted by Bennet *et al.*, and $k_v = -1.76$ MJ/m^3 which is larger than that for pure Co owing to the induced polarization of Pd by Co. In Co/Pd ML's with Pd buffer layer, t_{Co}^{tr} took place at 8.2 Å. θ_k was varied crucially according to t_{Pd}/t_{Co}, and their maximum value for our samples was 0.12°.

For (Pt(10Å) / Co(3Å)) x 15 / T_{Pt} MLs, surface roughness and H_c increased with increasing T_{Pt}. k_{eff} also increased for $T_{Pt} \leq 200$ Å. (Pt(10Å) / t_{Co}) x 15 / Pt(10Å) MLs showed a t_{Co}^{tr} of 4 Å. A self-manufactured Kerr spectrometer was employed to measure θ_k and R spectra from 450 to 850 nm of Co/Pt MLs. Larger θ_k was observed at larger t_{Co} and smaller T_{Pt}, and shorter wavelength. The highest reflectivity is observed at $T_{Pt} = 200$ Å, with a maximum of 78% at 650 nm. Figure of merit ($\sqrt{R}\,\theta_k$) of (Pt(10Å) / Co(3Å)) x 15 / T_{Pt} MLs was also evaluated to show the best figure of merit at 450 nm and a maximum of 0.19° at $T_{Pt} = 50$ Å.

ACKNOWLEDGMENTS

This work was supported in part by the Korean Science and Engineering Foundation through the Science Research Center of Excellence Program (1995), and also supported in part by the BSRI program of the Korean Ministry of Education under Contract No. BSRI-95-2406.

REFERENCES

1. P. F. Carcia, A. D. Meinhaldt, and A. Suna, Appl. Phys. Lett., 47, 178 (1985)
2. S. Hashimoto, Y. Ochiai, and K. Aso, J. Appl. Phys., 67 (4), 2136 (1990)
3. F. J. A. den Broeder, H. C. Donkersllot, H. J. G. Draaissma, and W. J. M. de Jonge, J. Appl. Phys., 61 (8), 4317 (1987)
4. W. B. Zeper, F. J. A. Greidanus, P. F. Carcia, and C. R. Fincher, J. Appl. Phys., 65 (12), 4971 (1989)
5. S. Tsunashima, M. Hasegawa, K. Nakamura, and S. Uchiyama, J. Magn. Magn. Mater., 93, 465 (1991)
6. C. J. Lin, G. L. Gorman, C. H. Lee, R. F. C. Farrow, E. E. Marinero, H. V. Do, H. Notarys, and C. J. Chien, J. Magn. Magn. Mater., 93, 194 (1991)
7. S. K. Kim, J. S. Kang, J. I. Jeong, J. H. Hong, Y. M. Koo, H. J. Shin, and Y. P. Lee, J. Appl. Phys., 72, 4986 (1992)
8. W. R. Bennet, C. D. England, D. C. Person, and C. M. Falco, J. Appl. Phys., 69 (8), 4384 (1991)